

# Simulation of a Ship Propulsion System Performance during Manoeuvring in Shallow Waters

Panagiotis Misythras\*, Christos Pollalis, Evangelos Boulogouris, Gerasimos Theotokatos

Naval Architecture, Ocean & Marine Engineering, University of Strathclyde  
Glasgow, Scotland, United Kingdom

## ABSTRACT

During initial ship design, a vessel's manoeuvrability and propulsion system performance are investigated separately, ignoring the interconnection that actually takes place in real conditions. In this paper, a new simulation tool has been developed by coupling the propulsion system and seakeeping models. The ship's manoeuvrability is investigated by using a non-linear 3-DOF manoeuvring model in calm water, whilst a mean value approach model is used for the simulation of the vessel's propulsion system performance. The main outcome of this method is to validate the simulation tool performance by using the available ship's turning circle sea trials and to simulate her performance and manoeuvrability in shallow water condition. The results include the consolidation of the ship trajectories and the performance of the propulsion system components during turning in various sea depths.

**KEY WORDS:** 3-DOF manoeuvring; propulsion system performance; engine response; shallow water.

## INTRODUCTION

Introduction of lower emission limits for the environmental protection stipulates the installation of more efficient systems. In the quest of the balance between efficiency and safety, IMO has recommended guidelines on the calculation of the minimum required installed propulsion power (IMO, 2013). According to these guidelines, the minimum power is estimated based on the propulsion system's performance that maintains the manoeuvrability of the ship.

Meanwhile, statistics indicate that the majority of the groundings and collisions in maritime world occur in coastal areas (EMSA, 2016). In such restricted areas, flow patterns changes, leading to alterations of ship's manoeuvring characteristics. Therefore, the manoeuvring behaviour of the ship, as well as the propulsion system performance during manoeuvring shall be investigated, identifying the interaction of the propulsion system performance to the ship's navigation during manoeuvring.

Due to the high cost of the sea trials and model tests, numerical methods have been developed for the estimation of the ship's trajectories and propulsion system performance, predicting the manoeuvrability of ships in calm water. These time – domain numerical simulation tools could be used from the early design stages of the ship in order to investigate whether it complies with the relevant IMO criteria and certify that the selected engine has adequate power.

The increase in ships' size in the last decades emerged the need to investigate manoeuvrability in shallow water. The distinction between deep water and shallow water is rather vague. However, in wave theory the shallow water is defined as the case when the ratio of water depth  $h$  to wave length  $\lambda$  is less than 4% ( $h/\lambda < 0.04$ ) (Lewis, 1989), whilst other studies give a more detailed distinction in navigational areas (MarCom, 1992). In general, it may be considered that when the ratio of water depth over vessel's draught is less than or equal to 2, then the sea bottom affects the hydrodynamic coefficients of the ship (van Oortmerssen, 1976). In the 23<sup>rd</sup> ITTC Manoeuvring Committee (ITTC, 2002), the model that was developed by the Manoeuvring Modelling Group (MMG) (Ogawa et al., 1977) has been reviewed in order to approximate the effect of the shallow water on the linear and nonlinear manoeuvring derivatives of the hull. For the ship's manoeuvrability prediction at the initial design stages, a practical calculation method has been developed, taking into account the hydrodynamic forces acting on the hull as functions of the main ship particulars (Inoue et al., 1981a).

The first model that was developed for the investigation of the interaction between the propulsion system and the propeller during manoeuvring was the 'Ship Mobility Model', using sub-models for the simulation of 4-stroke diesel engine, propeller and manoeuvring. The results of this model have been validated for an Air Defence and Command Frigate (Schulten, 2005), analysing the uncertainty and validity of complex simulation models (Schulten and Stapersma, 2007). Based on that model, a systematic modelling was developed and validated in dynamic conditions for a multi-purpose frigate, (Vrijdag et al., 2009).

Other efforts for the simulation of propulsion system during manoeuvring have focused on the simulation of the control system on board for a twin-screw ship (Martelli et al., 2014). In this paper, a six degree-of-freedom (DOF) model fully coupled with an engine performance simulation approach based on response surfaces was presented, able to simulate the ship's motions and trajectory. Similarly to the response surface, Shi et al. (2008) used a 3 DOF model and a simplified algorithm for the engine torque prediction to quantify the exhaust emissions during various ship voyage profiles.

In order to identify the interaction between the hydrodynamic performance of the ship and the performance of the propulsion system, CFD studies have been conducted to estimate the impact of the propulsion system on the propeller's thrust and torque (Boletis et al., 2015). In addition, the fluctuations of the two shaft line dynamics during manoeuvring have been investigated with the development of a simulator that predicts the interaction between a 3-DOF system and the propulsion system performance map (Viviani et al., 2008).

Other studies that focus mainly on the propulsion system, investigate the performance of the turbocharged engine during 'tip-in' manoeuvring, using a mean value approach model for the simulation of the main engine (Cieslar, 2013), or the effect of hybrid systems in manoeuvring condition (Dedes, 2013). Apart from the simulation of the propulsion system, experimental tests have been conducted for the estimation of the fluctuations during tight manoeuvres of a twin-screw ship (Mauro and Dubbioso 2012). Finally, the dynamic behaviour of a four-stroke, medium speed, marine diesel, driving a controllable pitch propeller has been investigated, using only the ship longitudinal motion equation for the prediction of ship's speed (Livanos et al., 2006).

Although numerous studies have been conducted for the ship manoeuvring simulation, they mostly focused on the propulsion system performance investigation in deep water conditions. Respective studies for the ship sailing in shallow waters have not been previously reported. Therefore, the main aim of this study is to investigate a tanker propulsion system response during manoeuvring in various sea depths. The time-domain numerical tool 'ELIGMOS' that simulates ship manoeuvring in calm water considering up to 4-DOF is used to calculate the ship turning ability in both deep and shallow water conditions (Pollalis et al., 2016). Based on the ship motion equations that refer to the horizontal plane, the instantaneous ship position, according to an earth-fixed coordinate system is identified by implementing a 4<sup>th</sup> order Runge-Kutta scheme. To allow the model predictive capability in restricted areas, the Ankudinov's empirical formulae (Ankudinov et al., 1990) are adopted for the estimation of the manoeuvring derivatives.

Additionally, the propulsion system performance of a two-stroke marine Diesel engine is simulated with a mean value approach model for investigating the propulsion system response during manoeuvring. The Mean value engine modelling approach was firstly introduced as a simplified method that uses the average values of engine performance parameters within one engine cycle (Woodward and Latorre, 1984). Since then, this model has been adopted for the prediction of marine diesel engine performance (Theotokatos, 2010) and for the estimation of the ship performance during acceleration in adverse sea conditions (Mizythras et al., 2016).

Based on the simulation of the ship's manoeuvrability in calm shallow water, the control parameters that affect the propulsion system response are investigated. Furthermore, the interaction between the simulation tools for the estimation of ship position, engine performance and navigation commands, is described.

## SIMULATION MODELS

### Ship Motions System

For the simulation of the ship's hydrodynamic performance, the numerical tool 'ELIGMOS', which was developed in C++ platform, is used. Assuming that the ship's speed during the turning motion is small and the vertical position of her centre of gravity is sufficiently low, resulting in negligible heeling moment, only the surge, sway and yaw motions are considered (3-DOF).

The applied mathematical model estimates the ship trajectories by use of two coordinate systems: the two-dimensional inertial system which is fixed at origin O and XY plane which always remains parallel to the undisturbed water surface, and the ship-fixed, M-xyz system, where M is located amidships and at the calm water surface level (Fig. 1). The estimation of ship's position refers only to the inertial, earth-fixed reference system.

The aforementioned, non-linear, 3-DOF mathematical model of surge, sway and yaw equations of motion is defined as follows (Pollalis et al., 2016):

$$(m' + m'_x)\ddot{u}' - (m' + m'_y)\dot{v}'r' - m'x'_G r'^2 = X' \quad (1)$$

$$(m' + m'_x)u'r' + (m' + m'_y)\dot{v}' + m'x'_G \dot{r}'^2 = Y' \quad (2)$$

$$(I'_N + J'_N)\ddot{r}' + m'x'_G(\dot{v}' + u'r') = N' \quad (3)$$

where  $m'$ ,  $I'_N$  are the non-dimensional mass and yaw moment of inertial of the ship,  $m'_x$ ,  $m'_y$ ,  $J'_N$  the non-dimensional surge and sway added masses and yaw added moment of inertia respectively. In addition,  $u' = u/U_o$ ,  $v' = v/U_o$  and  $r' = rL/U_o$  are the non-dimensional surge, sway and yaw velocities, whilst  $L$  is the ship's length and  $U_o$  is the initial speed during manoeuvring.

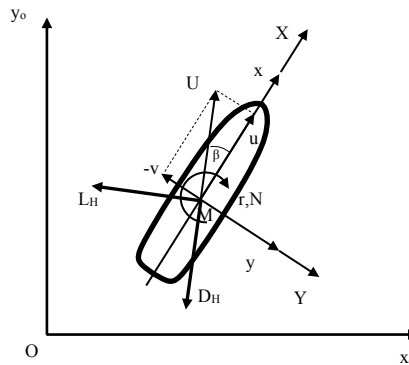


Fig. 1. Coordinate systems

The definition of the non-dimensional external surge and sway forces,  $X'$  and  $Y'$  respectively, and the non-dimensional external yaw moment  $N'$ , as well as the non-dimensional terms of ship mass, added masses and inertia are described in (Yasukawa et al., 2014). Added masses and inertia in yaw direction have been estimated from Motora's charts, based on the vessel's main particulars (Motora, 1960).

The lift ( $L_H$ ) and drag ( $D_H$ ) forces acting perpendicular and in the direction of the ship speed respectively, and their respective coefficients ( $c_L$ ,  $c_D$ ) are calculated as follows (Hooft, 1973):

$$L_H = X \sin \beta - Y \cos \beta, c_L = \frac{L_H}{0.5 \rho_{sw} U^2 L d} \quad (4)$$

$$D_H = -X \cos \beta - Y \sin \beta, c_D = \frac{D_H}{0.5 \rho_{sw} U^2 L d} \quad (5)$$

where  $\beta$  is the drift angle,  $\rho_{sw}$  is the sea water density and  $d$  is the vessel draught.

The hydrodynamic derivatives for the investigated case in surge, sway and yaw direction have been estimated by implementing the MMG method (Ogawa, A., 1977). For the estimation of hydrodynamic derivatives in shallow water, Ankudinov's method has been applied, which was derived from experimental data on various ship types (Vantorre, 2001; Ankudinov et al., 1990).

The effect of the shallow waters on ship's resistance  $R_o$  is considered as a function of sea depth over ship's draught (Furukawa et al., 2016):

$$\frac{[R_o]_{shallow}}{[R_o]_{deep}} = 0.388 \left( \frac{d}{h} \right)^2 + 1 \quad (6)$$

## Propulsion System Model

The investigated propulsion system consists of a two-stroke, turbocharged, marine Diesel engine, driving through the shafting system a fixed pitch propeller (PPP) (Fig. 2). The marine engine performance is simulated with the use of a computationally inexpensive mean value model, which was developed using MATLAB® programming language. The mean value approach uses average values of the engine's cycle, interconnecting the various components of the marine engine by using the mass and energy flow conservation equations (Theotokatos, 2010). The turbocharger of the propulsion system is simulated using an analytical expression that describes the steady state performance maps of the compressor and turbine, covering also the low speeds region of the compressor map (Mizythras et al., 2016).

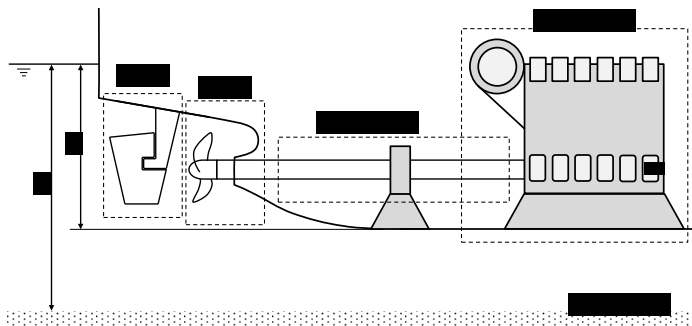


Fig. 2. Propulsion system plant

Based on the fuel flow rate and the combustion efficiency, the developed model estimates the indicated mean effective power of the engine. Taking into account the friction losses, the engine speed and the main dimensions of the engine, the produced power of the engine is calculated. The first thermodynamic law is applied for the estimation of the absorbed and produced power in the compressor and turbine elements respectively. Thus, the torque of the main engine ( $Q_E$ ), the compressor ( $Q_C$ ) and the turbine ( $Q_T$ ) are estimated using the respective shaft angular speed. The engine ( $n_E$ ) and the turbocharger shaft ( $n_{TC}$ ) rotational speeds are calculated according to the following differential equations derived by using the angular momentum conservation in the engine and turbocharger shaft respectively:

$$\frac{dn_E}{dt} = \frac{30(\eta_{sh} Q_E - Q_P)}{\pi(I_E + I_{sh} + I_{P\_tot})} \quad (7)$$

$$\frac{dn_{TC}}{dt} = \frac{30(Q_T - Q_C)}{\pi I_{TC}} \quad (8)$$

where  $Q_P$  is the propeller torque, and  $I_E$ ,  $I_{sh}$ ,  $I_{P\ tot}$  and  $I_{TC}$  are the inertias of engine, shafting system, propeller and turbocharger shaft respectively. The total inertia of the propeller includes the inertia of the propeller as if it was out of the water and the term of the added inertia due to the entrained water:

$$I_{P\_tot} = I_{P\_act} + I_{P\_entr} \quad (9)$$

The added inertia due to entrained water ( $I_{P\ entr}$ ) is calculated according to Lewis formula (Lewis, 1960).

The input variables for the engine simulation model include the engine speed and the rack position; the latter determines the fuel amount injected into the engine cylinders, which is controlled by the engine governor.

The engine governor is considered to be of the proportional-integral (PI type) requiring as input the ordered engine speed, which is a function of the vessel speed command. The developed engine governor model includes additionally the engine speed and torque limiters, as well as the engine speed slope limiter, used by the engine manufacturer to protect the engine integrity.

## Propeller Simulation Model

The torque and the thrust of the propeller are defined with the following corresponding formulae (Carlton, 2012):

$$Q_P = K_Q \rho_{sw} n_P^2 D_P^5, T_P = K_T \rho_{sw} n_P^2 D_P^4 \quad (10)$$

where  $\rho_{sw}$  is the sea water density,  $n_P$  is the propeller rotational speed and  $D_P$  is the propeller's diameter.  $K_Q$  and  $K_T$  are the torque and thrust coefficients, calculated as polynomial functions of the advance ratio.

The effect of the ship's turning motion on the flow pattern of the propeller is considered through the wake fraction  $w$  (Inoue et al., 1981b):

$$w = w_0 e^{K_w \beta_P^2} \quad (11)$$

where  $w_0$  is the wake fraction of the ship at initial conditions,  $K_w = -8.0$  and  $\beta_P$  is the inflow angle at the propeller position, derived by the formula (Hirano, 2009):

$$\beta_P = \beta - x'_P r' \quad (12)$$

## Simulation System

The integrated simulation system couples 'ELIGMOS' with the Propulsion System Performance Simulator and runs in MATLAB®. At each time step, 'ELIGMOS' estimates the new position of the ship, giving the velocity of the ship as input to the Propulsion System Simulator. Simultaneously, the Propulsion System Simulator calculates the propulsion system parameters and estimates the new engine speed and load. Considering that the engine drives a fixed pitch propeller, the propeller speed is estimated and is given as input to the Propeller Simulation System for the estimation of the propeller thrust and torque.

Then, the propeller thrust is utilized by ‘ELIGMOS’, identifying the new position of the vessel using a Runge-Kutta 4<sup>th</sup> order integration scheme. The propeller characteristics, as well as the wake fraction data are shared between the simulators.

## SIMULATION RESULTS

In this section, the derived results are presented. First, the validation process of the coupled simulators is described, and subsequently, the simulation results of the investigated vessel manoeuvring in deep water and two different cases of shallow waters are presented and discussed.

### Validation Process

The developed simulation tool has been validated for an oil tanker. The non-dimensional ratios of the oil tanker are given in Table 1. The vessel is equipped with a two-stroke, turbocharged engine, driving an FPP through the shafting system.

Table 1. Ship data

Main particular ratios	
L/B	5.46
B/d	2.93
Block coefficient $c_b$	0.84
Admiralty Coefficient	835.64

According to the non-dimensional sea trials data, the simulation tool has been validated for the propulsion performance during turning circle manoeuvring in both port and starboard directions. Constant rudder’s turning rate is considered until a maximum value of 35°. The comparison of the ship trajectories between the simulation tool results and the ship data are given in Fig. 3. The simulation results agree very well with the test results for the turning motion, satisfying advance, transfer and tactical diameter of the available data.

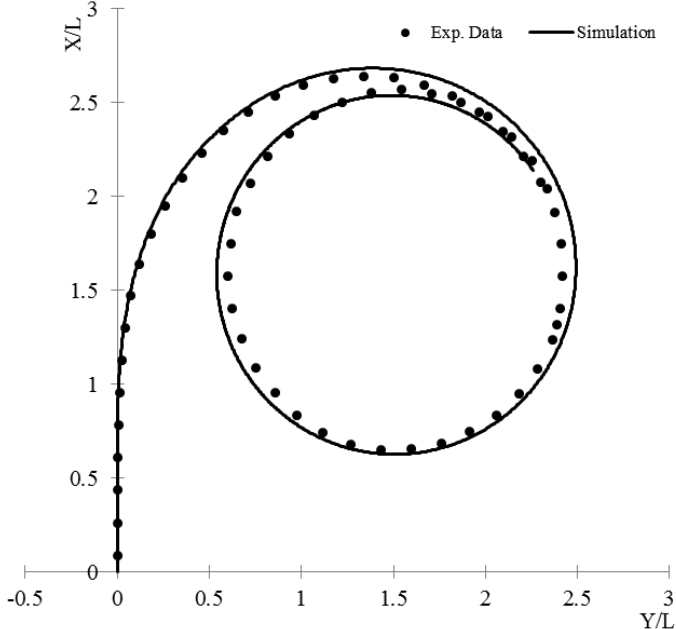


Fig. 3. Comparison between the results of the simulation tool and the available sea trials data.

In order to predict the speed profile of the ship during manoeuvring, the engine speed control unit is used in the simulation tool. In all the performed runs, the ordered engine speed was set to the maximum continuous rating point (MCR). Then, the engine speed is calculated according to Eq. 7 and is used to estimate the propeller performance. After the engine load and speed have been determined by the propulsion system module, ‘ELIGMOS’ calculates the vessel’s speed. Then, the Froude number at each position of the ship’s trajectory is calculated and compared with the available data as shown in Fig. 4.

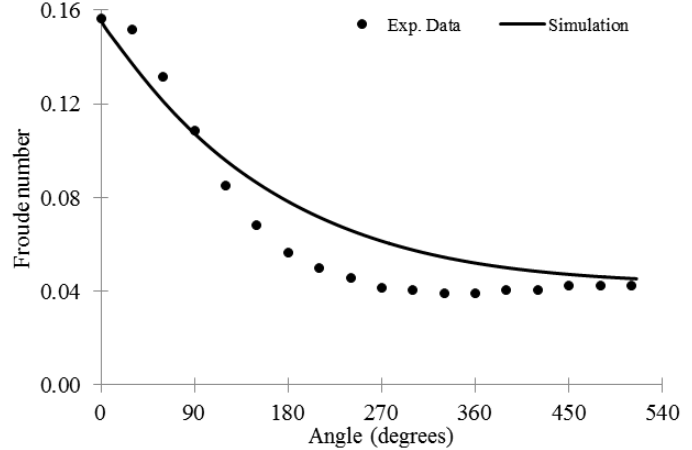


Fig. 4. Comparison between simulations results and data of the Froude number during vessel’s manoeuvring

As shown in Fig. 4, the ship decelerates faster during the start of the turning circle than the simulation tool predicts. The faster deceleration may be attributed to the faster variation of the propeller rotational speed or due to differences between the actual and the model’s ordered engine/propeller speed profile during manoeuvring. Thus, the temporal evolution of ship’s manoeuvring in real conditions is considered slower than the predicted. However, the validation process indicates that the developed tool simulates quite adequately the position and the speed of the vessel during the turning motion.

Table 2. Validation results of propulsion system simulation in various loads.

Engine Load	25%	50%	75%	100%
Brake Power (kW)	0.03%	-0.02%	-0.02%	0.28%
BSFC (gr/kWh)	0.99%	-0.20%	0.31%	-0.04%
T/C Speed	5.06%	2.16%	0.15%	-0.03%
SR Temperature (K)	-2.03%	-0.13%	-3.11%	-3.80%
ER Temperature (K)	2.06%	-0.95%	0.90%	1.12%
Compressor pressure ratio	1.49%	2.43%	-0.27%	-0.55%
Turbine pressure ratio	-2.73%	1.33%	-0.47%	0.10%

The validation of the propulsion system performance prediction module was performed by calculating the main engine parameters for a variety of loads, considering that the engine operates at steady state conditions (constant speed and rack position) and comparing them against its shop trial tests. The maximum error of the validation process for the propulsion system operation is less than 5% (Table 2).

The validation process indicates that the tool provides a very sufficient overall estimation of the propulsion system performance in steady-state conditions. As long as the correct shaft and propeller inertias are provided to the propulsion system simulator, the tool is valid to be used in transient conditions (Theotokatos, 2010).

## Simulation in Deep and Shallow Waters

The vessel's manoeuvrability during turning motion is simulated for three different water depths. The first condition describes the manoeuvring simulation in deep water condition (DW), namely  $h/d > 3.0$ , the second condition refers to shallow water (SW) with a ratio of sea depth over ship's draught equal to  $h/d = 1.5$ , whilst the third condition considers very shallow water ( $h/d = 1.2$ ). Each time, the simulation is performed by setting the maximum turning angle of the rudder in starboard and portside direction. Based on the simulation results, the trajectories of the ship and the performance of the propulsion system in each condition are compared.

In all cases, the ordered engine speed is equal to the MCR engine speed, whilst the considered water depth is defined as aforementioned. Therefore, the manoeuvring derivatives and the hydrodynamic coefficients of the investigated vessel are modified accordingly. The simulation time is 12 minutes in each case, indicating the impact of the sea depth on the ship's manoeuvrability and performance ability. The initial rotational speed of the engine is constant for all the investigated cases (106 rev/s). Consequently, when the simulation starts, the propulsion system performance and the vessel's speed are in equilibrium. For the investigation and discussion of the propulsion system parameters during manoeuvring, only the data during starboard turning circle simulations is used.

When the vessel is sailing in shallow water, the turning circle manoeuvring characteristics, namely advance, transfer and tactical diameter, increase (Fig. 5). This agrees with the conclusions of other researchers (Yasakawa et al., 2014). A comparison of the advance ( $D_a$ ), tactical ( $D_t$ ) diameter and transfer ( $D_{tr}$ ) non-dimensional values are presented in Table 3. The variation of the vessel speed, as well as the drag and lift forces that apply on the full are demonstrated in Figs. 6~7.

Table 3. Comparison of advance, tactical and transfer diameters in deep and shallow water conditions during starboard manoeuvring.

Sea water depth	Deep $h/d > 3.0$	Shallow $h/d = 1.5$	Shallow $h/d = 1.2$
$D_a/L$	2.68	3.39	4.78
$D_t/L$	2.49	2.96	3.49
$D_{tr}/L$	1.39	1.79	2.44

As it is shown in Fig. 6, the initial speed is decreased as the sea depth decreases due to the increase of the total resistance. During manoeuvring, the lift and drag coefficients decrease when the distance of the keel from the sea bottom decreases (Fig. 7). Thoroughly, the reduction of the drag coefficient leads to a lower speed loss in shallower water (Fig. 6), whilst the reduction of the lift coefficient explains the increase of the turning cycle diameter when the sea depth decreases. The increase of the turning diameters, vessel speeds and hydrodynamic forces acting on the hull in shallower waters is confirmed from previous studies (Hooft, 1973).

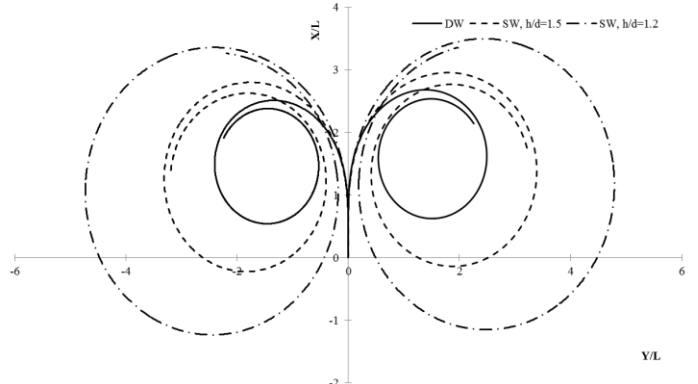


Fig. 5. Vessel trajectory in deep (DW) and shallow (SW) sea water conditions

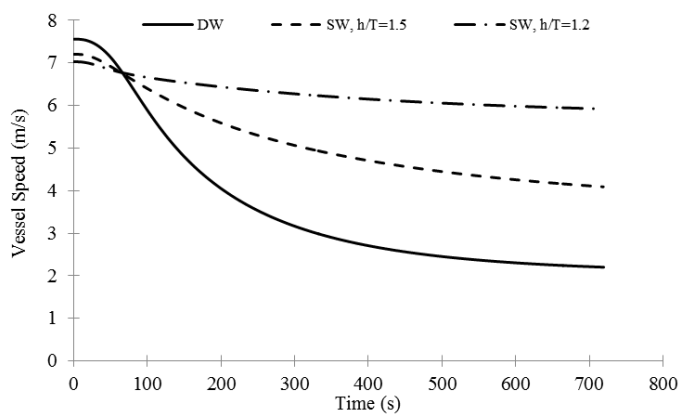


Fig. 6. Comparison of vessel speed time diagrams in deep (DW) and shallow (SW) sea water conditions.

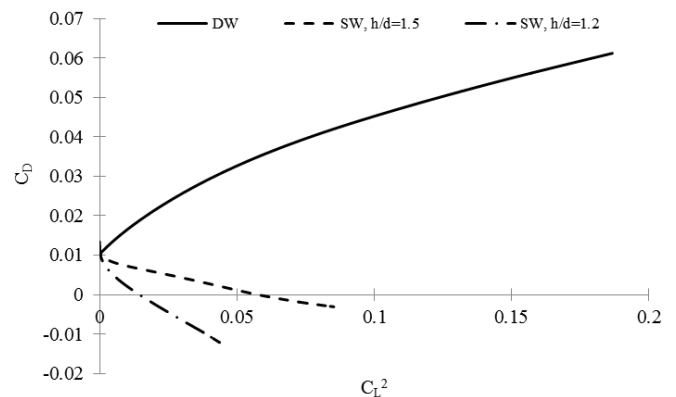


Fig. 7. Comparison of lift and drag coefficients in deep (DW) and shallow (SW) sea water conditions.

The engine – propeller interaction and the performance of the propulsion system is shown in Figs. 8~11. In specific, the change of the fuel rack position that controls the amount of the injected fuel into the engine cylinders is presented and compared with the alteration of the engine speed percentage. Moreover, some main engine performance parameters, such as the break specific fuel consumption, the break mean effective power, the scavenging receiver pressure and the temperature in the exhaust gas receiver are presented.

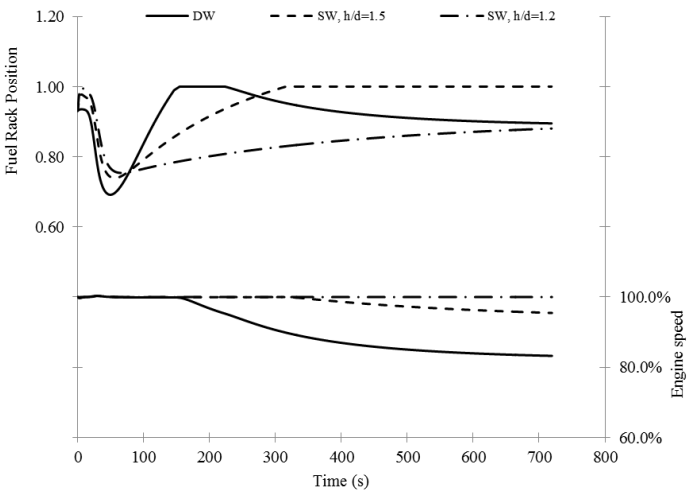


Fig. 8. Comparison of fuel rack position and engine speed time diagrams in deep (DW) and shallow (SW) sea water conditions.

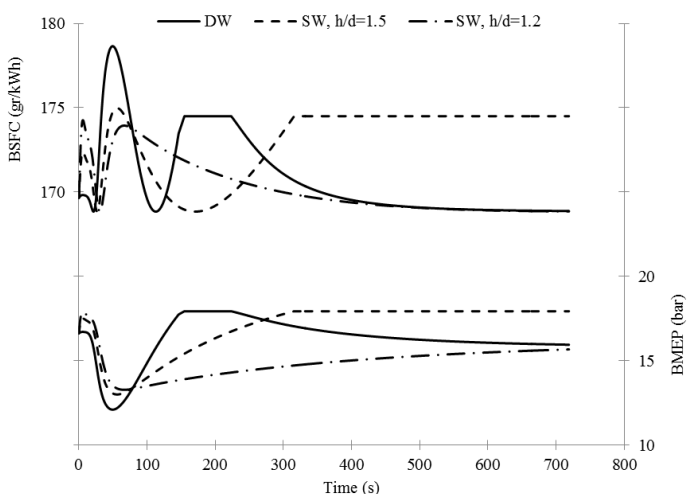


Fig. 9. Comparison of break mean effective power (BMEP) and break specific fuel consumption (BSFC) time diagrams in deep (DW) and shallow (SW) sea water conditions.

In Fig. 8, the variations of the fuel rack position and engine speed are presented for the three investigated cases. During the first seconds of the deep water simulation and while rudder is turning to the maximum permitted angle, there is a delay in the engine's response. Following the rudder turning, the propeller effective wake is varying, decreasing the wake fraction of the ship due to the inflow angle increase (Eq. 12). As a result, the advance speed of the propeller increases which leads to a reduction of propeller's torque. Thus, the engine governor reduces the fuel rack position in order to keep the propeller speed equal to the ordered speed from the control unit. When the variation of the effective wake profile of the propeller is stabilized (minimum wake fraction), the propeller torque and thrust are considerably increased, increasing simultaneously the power demand from the engine and the fuel rack position until the maximum allowable value from the fuel governor limiters (100% at the beginning), in order to achieve the ordered engine speed. Therefore, the fuel governor follows the torque limiter curve till the end of the manoeuvring simulation.

While the ship is turning, the forces on the hull increase, resulting in a reduction of the vessel's speed and increasing simultaneously the propeller's torque. Due to the activation of governor's torque limiter, the fuel flow rate is also limited to the maximum permitted. Therefore, the main engine operates at its maximum load for a considerable period during ship manoeuvring. Due to the greater propeller power demand in comparison to the engine power supply, the engine/propeller speed reduces. In addition, the overall speed of the vessel also reduces as the resistance exceeds the propeller produced thrust.

In general, it can be noticed that the forces acting on the hull affect the performance of the propulsion system. When the sea depth decreases to  $h/d=1.5$ , the drag force is reduced. As a result, the engine is able to keep the ordered speed for longer time until the engine limiter will be activated. Due to the higher engine speed, the engine torque limiter allows the governor to be set to the maximum fuel rack position (100%). When the depth of the sea water is further decreased ( $h/d=1.2$ ), the drag and lift forces acting on the hull reduce even more. Thus, the engine load decreases, reducing the fuel consumption and the produced torque. As a result, the sea depth affects the performance of the engine in restricted areas.

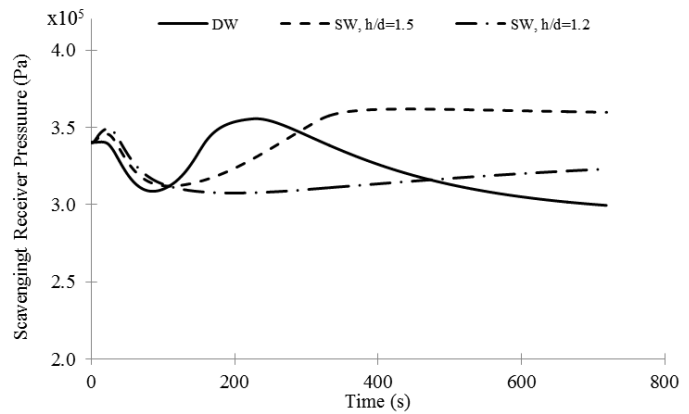


Fig. 10. Comparison of scavenging receiver pressure time diagrams in deep (DW) and shallow (SW) sea water conditions.

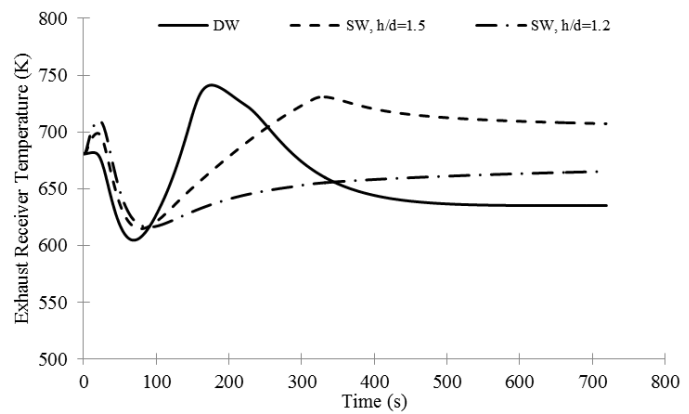


Fig. 11. Comparison of exhaust receiver temperature time diagrams in deep (DW) and shallow (SW) sea water conditions.

Furthermore, the activation of the engine limiter affects the operation of the propulsion system as it is depicted in the Figs. 9~11. The most representative indicators of main engine's performance are the break mean effective power (BMEP) and the break specific fuel consumption (BSFC). In each case, the BSFC and BMEP vary due to the different sea conditions. Shallower water increases the delivered torque from the engine at the initial conditions due to the increased resistance.

At the beginning of manoeuvring, the engine load reduces due to the variation of effective wake profile from the rudder turning, decreasing the BMEP. When the effective wake profile is stabilized, the propeller thrust and torque increase, increasing the BMEP. The power increase in each case is different due to the varying drag forces acting on the hull. In the case of the deep water and shallow water, the engine approaches the limiters, defining the delivered work of the engine. On the other hand, no limiters are activated during the manoeuvring in very shallow water. When the turning motion starts, there is an excess of thrust from the propeller at the initial speed. As a result, the governor reduces the fuel mass flow rate to the engine, reducing the BMEP. When the balance between thrust and resistance is restored, the BMEP is stabilized. The engine operating point affects the specific consumption respectively. Even if the BMEP and BSFC values in both deep and very shallow water cases are the same, the engine speed is different (Fig. 8), indicating that when the ship manoeuvres in deep water, the engine performs at the engine torque limit.

The time variations of the scavenging receiver pressure (Fig. 10) and the temperature in the exhaust receiver (Fig. 11) follow the engine load variation. At the beginning of ship's turning circle, the pressure and temperature remain constant due to the relevant steady state conditions of the engine operation. Subsequently, as the engine load decreases, there is a drop in the boost pressure and the exhaust gas temperature, whilst the flow parameters increase when the propeller load increases as well.

As aforementioned, the maximum temperature and pressure of the receivers are affected by the limiters that are applied on the engine by the fuel governor. However, the maximum values are different in each studied case. At shallow water conditions and higher vessel speeds, the pressure in the scavenging receiver remains high for longer time, proving that the turbocharger operates in higher speeds in order to provide the required air flow rate to the engine. As shown in Fig. 10 the scavenging pressure is still high even if the engine power is reduced in very shallow waters due to the higher engine speed.

An increased engine thermal loading can be inferred from the exhaust receiver temperature plots, as the exhaust gas temperature remains close to its maximum values for the longer period during the manoeuvres at shallow waters. The engine operation at higher speeds results in greater levels of turbocharger speed and the pressure in the scavenge air receiver.

The time variations of the propulsion system parameters indicate that when the vessel sails from deep to shallow waters, the engine power is increased, close to its maximum load, in order to cover the ordered speed from the governor. However, when the ship sails in very shallow water, the reduction of the drag forces applying on the hull is significant, reducing the fuel consumption of the engine. Despite the variations of propulsion system performance, the decrease of the sea's depth increases the transfer and tactical diameters of the ship during manoeuvring. As a result, the thorough investigation of ship manoeuvring in shallow waters during the preliminary ship design phase is critical for the appropriate selection of the ship main engine MCR, revealing the necessity of the application and further

development of the recommended guidelines for the determination of the minimum required propulsion power.

## CONCLUSIONS

In this study, the performance of a ship's propulsion system is investigated during a turning circle manoeuvre. The investigation includes the identification of the ship trajectory in deep and shallow water depth and the effect that the sea depth has on the ship's manoeuvrability. The investigation has been performed using an oil tanker which is equipped with a two-stroke marine diesel engine, driving a fixed pitch propeller.

The validation process proved that the developed tools are able to provide adequate accuracy concerning the simulation of propulsion system hydrodynamic performance. The simulation tool for the propulsion system was validated independently. Then, the coupled simulation tool was verified with the available ship's trajectory by setting a specific speed order to the fuel governor control unit which was incorporated in the propulsion system tool. The comparison between simulation results and available data indicates that the tool provides adequate estimation of the ship's position and speed.

The aforementioned validated tools were used for the simulation of the ship's performance in three different conditions: navigation in deep water and navigation in two different shallow water conditions. The results of the simulation provided useful and practical insight on the performance of the propulsion system during manoeuvring. When the water depth reduces, the characteristic manoeuvring values of the ship, namely advance, transfer and tactical diameter increase, showing that the alteration of the flow characteristics in shallow water lead to poor manoeuvrability. Such a result is important especially as the ability of a ship to avoid obstacles is decreased when she sails in restricted areas. Considering also that the initial conditions during simulations have been set to the maximum delivered engine speed and load, the forces on the hull and the rudder are the maximum that can be developed.

Apart from the ship's trajectory, the simulation of the propulsion system's performance indicates the effect of the engine components on the ship's hydrodynamic performance. The detailed simulation of the turbocharger, engine and propulsion systems proves that the limiters affect the vessel's speed and consequently the developed forces on the ship.

When the turning order is given to the rudder, there is a delay on the propulsion system in order to detect this modification of the effective wake profile at the propeller. As a result, there is a slight decrease on the delivered power from the engine. Therefore, the power variation depends on the propeller's demand. In deep and shallow water, power increases to its maximum value permitted from the propulsion system limiters. On the other hand, the reduction of the propeller thrust in very shallow water, reduces the produced power from the engine. However, the validation of the simulation results is impossible in lack of the engine performance data in transient conditions.

Additionally, the interaction between the applied forces on vessel's hull and the propulsion system indicate that the limiters that are applied on the engine, as well as the control unit, have great impact on the ship's manoeuvrability. Further investigation of the engine limiters and their application on the propulsion system could provide a better insight on their effect to the overall ship's performance during turning motion.

Finally, the simulation revealed the dynamic interaction between the sea environment and the propulsion system of the ship. During

manoeuvring, the worst condition of shallow water shall be identified, investigating the sea depth that requires the maximum power from the propulsion system, leading the engine's performance on the limit. Therefore, the operation of the ship shall be further investigated in dynamic and transient conditions, where the power demands increase and limiters are activated for the protection of the propulsion system.

## ACKNOWLEDGEMENTS

This work was partially supported by the "HOLISHIP – Holistic Optimisation of Ship Design and Operation for Life Cycle" project that which was funded from the European Union's Horizon 2020 research and innovation programme under grant agreement N° 689074.

## REFERENCES

- Ankudinov, V.K., Miller, E.R., Jakobsen, B.K., and Daggett, L.L. (1990). "Maneuvering Performance of Tug/Barge Assemblies in Restricted Waterways," *Proc. MARSIM & ICMS 90*, Tokyo, Japan, 512-525.
- Boletis, E., de Lange, R., and Bulten, N. (2015). "Impact of Propulsion System Integration and Controls on the Vessel DP and Manoeuvring Capability," *IFAC-PapersOnLine*, 48-16, 160-165.
- Carlton, J.S. (2012). "Marine Propellers and Propulsion," *Butterworth-Heinemann*.
- Cieslar, D. (2013). "Control for Transient Response of Turbocharged Engines", *PhD Thesis*, University of Cambridge – Department of Engineering, UK.
- Dedes, E. (2013), "Investigation of Hybrid Systems for Diesel Powered Ships," *PhD Thesis*, University of Southampton – Faculty of Engineering and the Environment, UK.
- EMSA (2016), "Annual Overview of Marine Casualties and Incidents 2016".
- Furukawa, Y., Ibaragi, H., Nakiri, Y., and Kijima, K. (2016). "Shallow Water Effects on Longitudinal Components of Hydrodynamic Derivatives," *Proc. 4<sup>th</sup> MASHCON*, Hamburg, Germany, 295-303.
- Hirano, M. (2009). "On Calculation Method of Ship Maneuvering Motion at Initial Design Phase," *Journal of the Society of Naval Architects of Japan*, 1980(147), 144-153.
- Hooft, J.P. (1973). "Manoeuvring Large Ships in Shallow Water – I," *Journal of Navigation*, 26(02), 189-201.
- IMO (2013), "2013 Interim Guidelines for Determining Minimum Propulsion Power to Maintain the Manoeuvrability of Ships in Adverse Conditions," *The Marine Environment Protection Committee, Resolution MEPC.232(65)*.
- Inoue, S., Hirano, M., and Kijima, K. (1981a). "Hydrodynamic Derivatives on Ship Manoeuvring," *International Shipping Progress*, 28 (321).
- Inoue, S., Hirano, M., Kijima, K., and Takashima, J. (1981b). "A Practical Calculation Method of Ship Maneuvering Motion," *International Shipping Progress*, 28 (325).
- ITTC, (2002). "Report of the Manoeuvring Committee," *Proceedings of the 23<sup>rd</sup> International Towing Tank Conference*, I, 153-200.
- Lewis E.V. (Editor), (1989), "Principles of Naval Architecture-2<sup>nd</sup> Edition", Vol. III, Society of Naval Architects and Marine Engineers, ISBN No. 0-939773-02-3.
- Lewis, F.M., and Auslaender, J. (1960). "Virtual Inertia of Propellers," *Journal of Ship Research*, 3(4), 37-46.
- Livanos, G.A., Simotas, G.N., Dimopoulos, G.G., and Kyrtatos, N.P. (2006). "Simulation of Marine Diesel Engine Propulsion System Dynamics during Extreme Maneuvering," *ASME International Combustion Engine Division Technical Conference*, Aachen, Germany.
- MarCom, (1992). "Capability of Ship Manoeuvring Simulation Models for Approach Channels and Fairways in Harbours," *Report of Working Group 20 of Permanent Technical Committee II*, Supplement to PIANK Bulletin No. 77, 49.
- Martelli, M., Viviani, M., Altosole, M., Figari, M., and Vignolo, S. (2014). "Numerical Modelling of Propulsion, Control and Ship Motions in 6 Degrees of Freedom," *J. Engineering for the Maritime Environment*, 228(4), 373-397.
- Mauro, S., and Dubbioso, G. (2012). "Influence of Propulsion System Configuration on the Manoeuvring Performance by Free Running Model Tests," *Proc. 9<sup>th</sup> IFAC Conference on Manoeuvring and Control of Marine Craft*, Arenzano, Italy, 31-36.
- Mizythras, P., Boulogouris, E., and Theotokatos, G. (2016), "Computational Investigation of Ship Propulsion Performance in Rough Seas," *Proc. International Conference on Maritime Safety and Operations*, Glasgow, UK, 183-193.
- Motora, S. (1960). "On the Measurement of Added Mass and Added Moment of Inertia for Ship Motions," *Journal of Zosen Kiokai*, 106.
- Ogawa, A., Koyama, T., and Kijima K. (1977). "MMG report-I, On the Mathematical Model of Ship Manoeuvring," *Bulletin of Society of Naval Architectures of Japan*, 575, 22-28.
- Pollalis, C., Boulogouris, E., Turan, O., and Incecik, A. (2016), "ELIGMOS: Time Domain Simulation of the Manoeuvring of Ships in Deep and Shallow Waters," *Proc. International Conference on Maritime Safety and Operations*, Glasgow, UK, 211-216.
- Schulten, P.J.M. (2005). "The interaction between diesel engines, ship and propellers during manoeuvring," *PhD Thesis*, Technische Universiteit Delft, Netherlands.
- Schulten, P.J.M. and Stapersma, D. (2007). "A study of the validity of a complex simulation model," *Proc. of the Institute of Marine Engineering, Science and Technology Part A: Journal of Marine Engineering and Technology*, (10), 67-77.
- Shi, W., Stapersma, D., and Grimmelius, H. (2009). "Simulation of the influence of ship voyage profiles on exhaust emissions," *ASME, Proc of International Mechanical Engineering Congress and Exposition*, 14, 164-174.
- Theotokatos, G. (2010). "On the Cycle Mean Value Modelling of a Large Two-Stroke Marine Diesel Engine," *Proc. Of the Institution of Mechanical Engineers, Part M: Journal of Engineering for the Maritime Environment*, 224(3), 193-205.
- van Oortmerssen, G. (1976). "The Motions of a Ship in Shallow Water," *Ocean Engineering*, 3, 221-255.
- Vantorre, M. (2001). "Manoeuvring Coefficients for a Container Carrier in Shallow Water: An Evaluation of Semi-Empirical Formulae," *Mini-Symposium on Prediction of Ship Manoeuvring Performance*, Tokyo, Japan, 71-81.
- Viviani, M., Altosole, M., Cerruti, M., Menna, A., and Dubbioso, G. (2008). "Marine Propulsion System Dynamics During Ship Manoeuvres," *6<sup>th</sup> International conference on high-performance marine vehicles*, Naples, Italy, HIPER, 18(19).
- Vrijdag, A., Stapersma, D., and Van Terwisga, T. (2009). "Systematic modelling, verification, calibration and validation of a ship propulsion simulation model," *Proc. of the Institute of Marine Engineering, Science and Technology Part A: Journal of Marine Engineering and Technology*, (15), 3-20.
- Woodward, J.B., and Latorre, R.G. (1984). "Modeling of Diesel Engine Transient Behavior in Marine Propulsion Analysis," *SNAME Transactions*, 92, 33-49.
- Yasukawa, H., and Sano, M. (2014). "Maneuvering Prediction of a KVLCC2 Model in Shallow Water by a Combination of EFD and CFD," *Workshop on Verification and Validation of Ship Manoeuvring Simulation Methods*, Force Technology, Copenhagen.